

# 1 *In situ* Methanation on Mars: A Process Concept Study 2 on the Impact of H<sub>2</sub>/CO<sub>2</sub> and Recycle Ratio

3 Franz Braun<sup>1</sup>, Thomas-Oliver Nagel<sup>1</sup>, Samuel Prinz<sup>1</sup>, Jens Friedland<sup>1</sup>, Robert Güttel<sup>1\*</sup>

4 <sup>1</sup>Institute for Chemical Engineering, Ulm University, Albert-Einstein-Allee 11, 89081 Ulm,  
5 Germany.

6 \*corresponding author: robert.guettel@uni-ulm.de

## 7 Abstract

8 For planning return missions from Mars, considerations about the supply of rocket fuel are  
9 crucial. Since transportation of propellant from Earth and storage at Mars is costly and energy  
10 intensive, *in situ* resource utilization (ISRU) for methane production on Mars presents a  
11 promising solution. The major challenge is to identify a simple and robust production process,  
12 which provides the required purity of the propellant. In this study, we compare two different  
13 process concepts, with and without recycle, under realistic operating conditions using  
14 thermodynamic modelling and simulation. The H<sub>2</sub>/CO<sub>2</sub> feed ratio is crucial to achieve  
15 sufficiently high methane selectivity and thereby reduce the effort in product gas cleaning and  
16 the overall process complexity. At the same time, recycling unreacted reactants reduces  
17 resource consumption, which is preferable for ISRU scenarios. Hence, our study provides a  
18 basis for more detailed process design using kinetic information on the involved process steps.

## 19 Keywords

20 Methanation, *in situ* resource utilization, H<sub>2</sub>/CO<sub>2</sub> feed ratio, modelling, simulation, recycle,  
21 ISRU, Mars

## 22 1 Introduction

23 Human missions to Mars are a significant subject owing to NASA's and SpaceX's vast efforts  
24 to accomplish them within the next few decades. The establishment of return missions is a

25 crucial prerequisite for the recovery of human life after successful Mars missions. The most  
26 promising strategy is the utilization of a Mars ascent vehicle (MAV) for transfer between the  
27 surface and the orbit of Mars, while the transport between Mars orbit and earth is realized via  
28 an earth return vehicle (ERV) [1]. The required fuel for the launch into the Mars orbit via MAV  
29 can either be carried from earth and stored at the Mars surface or it can be produced on Mars.  
30 The latter concept of *in situ* resource utilization (ISRU) has been introduced already in the  
31 1980s [2].

32 In the 1990s elaborate plans have been made on how Mars missions can profit from ISRU  
33 technology in the Design Reference Missions (DRMs) [3]: By producing propellant *in situ* on  
34 Mars, the start mass of the mission and the mass of the lander vehicle can be significantly  
35 reduced [3]. Furthermore, *in situ* propellant production provides more flexible surface  
36 exploration capability and the possibility of longer mission durations due to the possibility of  
37 refuelling rovers [3]. In addition, longer mission durations reduce the mission risk due to fewer  
38 launches [3]. It is even conceivable that the necessity for live supporting facilities may become  
39 redundant [3]. For example, ISRU systems include the production of O<sub>2</sub> via electrolysis [4,5],  
40 which can provide O<sub>2</sub> for the human habitat in the event of leaking O<sub>2</sub> tanks. Nevertheless,  
41 ISRU does require higher energy input to support the operation of the required process units,  
42 including compressors, electrolysis, heat exchangers, excavators, haulers, and so forth [3]. In  
43 addition, the employed systems must be capable of long service life, since equipment  
44 replacement requires costly transport missions from earth [3]. The DRM outlines two distinct  
45 mission scenarios for a prolonged human stay on Mars: 1. A single site habitat for human  
46 presence in combination with multiple exploration missions and 2. several habitat sites during  
47 multiple Mars missions [3]. The latter scenario necessitates the construction of multiple  
48 facilities with the required infrastructure including potential ISRU capabilities.

49 Methane synthesis from H<sub>2</sub> and CO<sub>2</sub>, also referred to as CO<sub>2</sub> methanation, is a well-established  
50 process on Earth [6–8]. The main reaction is depicted in eq. (RE1). However, unwanted side  
51 reactions may lead to the formation of CO (RE2), while CO can also be hydrogenated to

52 methane (RE3). Depending on the operating conditions, in particular temperature, pressure  
53 and gas composition, and the choice of catalyst, the by-product formation can be reduced.



54 The CO<sub>2</sub> hydrogenation reactions are typically performed in fixed-bed reactors using Ni-based  
55 porous solid catalysts. The major challenge is the exothermic nature of the reaction and the  
56 limitation of conversion due to thermodynamic constraints. Therefore, industrial scale plants  
57 (e.g., from Air Liquide and Haldor Topsøe) use a cascade of adiabatic fixed-bed reactors with  
58 intermediate cooling or the partial recycling of product streams for heat integration and removal  
59 of the released reaction heat [6]. Furthermore, the recycle possess an additional degree of  
60 freedom in process operation, which provides improved flexibility in particular for dynamic  
61 operation [9,10]. In order to push the thermodynamic constraints, the operation under over-  
62 stoichiometric H<sub>2</sub>/CO<sub>2</sub> feed ratios appears to be a promising concept, as evidenced by literature  
63 [11–14]. This method is particularly suitable for ISRU, since it is easily feasible without of  
64 additional unit operations [11,13].

65 In recent years, NASA has conducted experiments aiming to develop ISRU technologies. In  
66 one such experiment, the Martian atmosphere was simulated with an Atmospheric Processing  
67 Module as part of the MARCO POLO (Mars Atmospheric and Regolith Collector/Processing  
68 for Lander Operations) project [14–16]. The CO<sub>2</sub> was collected via a freezer and subsequently  
69 hydrogenated using 88 g of a 0.5 wt-% ruthenium on alumina catalyst to methane in a Sabatier  
70 reactor [16]. During the initial start-up phase, hydrogen was supplied in excess of the  
71 stoichiometric ratio (4.5:1) [15,16]. The unreacted hydrogen is recovered via a membrane and  
72 returned to the reactor with some methane. After the start-up phase, the system inlet  
73 composition is reduced to the stoichiometric H<sub>2</sub>/CO<sub>2</sub> ratio of 4:1. Due to the recycling of  
74 unreacted H<sub>2</sub>, the reactor inlet H<sub>2</sub>/CO<sub>2</sub> ratio exceeds the stoichiometric value of 4:1. However,  
75 no further specification is provided regarding the precise H<sub>2</sub>/CO<sub>2</sub> ratio at the reactor inlet. With  
76 a CO<sub>2</sub> conversion of 99.9% at a reaction temperature of 450°C the system demonstrates the

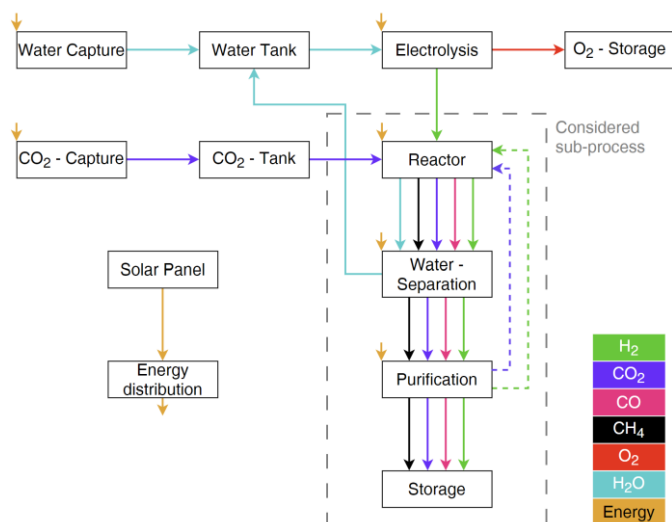
77 production of 32 g h<sup>-1</sup> methane with a purity of 99.9% [14,15]. Apart from that, an investigation  
78 into the impact of the H<sub>2</sub>/CO<sub>2</sub> ratios on CO<sub>2</sub> conversion and product purity has not been  
79 included in the research's scope. Furthermore, a Sabatier reactor system is currently  
80 undergoing testing on the International Space Station (ISS) as part of the oxygen recovery  
81 system. This system is designed to convert the CO<sub>2</sub> produced by astronauts into methane and  
82 water [14]. The details of the final version of the system are not yet available. Nonetheless,  
83 information pertaining to a developmental version has been made public by NASA [14,17].  
84 A noteworthy first extraterrestrial ISRU demonstration is conducted with MOXIE, which is an  
85 oxygen production system and component of the Mars rover Perseverance [18]. Hoffman et  
86 al. [18] report that seven experiments under both diurnal and nocturnal conditions yielded 50 g  
87 of oxygen produced from CO<sub>2</sub> in the Martian atmosphere. Thus, experimental demonstration  
88 of the feasibility of ISRU at operating conditions at day and night is achieved. A further goal is  
89 the demonstration of *in situ* oxygen production with MOXIE during different Martian seasons  
90 with different ambient atmospheric pressures from 631 Pa to 757 Pa [18]. Another promising  
91 concept for ISRU oxygen production is the pyrolysis of regolith, as demonstrated for lunar  
92 regolith by Šeško et al. [19].  
93 A proposed timeline for Mars missions, as outlined by NASA, includes a 16-months period for  
94 propellant production in order to provide 7 metric tons of methane, which is required for the  
95 return mission [20]. The resulting daily methane production target is  $\dot{n}_{\text{CH}_4} = 0.91 \text{ kmol d}^{-1}$ .  
96 Alam et al. [20] proposed a concept for production of the required amounts of methane based  
97 on available experimental and simulated data. The concept was assessed at a single operation  
98 point only and assumes experimentally proven CO<sub>2</sub> conversions of 60% and CH<sub>4</sub> selectivities  
99 of 99.5% While the work clearly demonstrates the general feasibility of methane production via  
100 ISRU, the underlying model is too simple to evaluate the impact of operation conditions on the  
101 yield and purity of the products. The oversimplification also holds for the separation units  
102 required to provide sufficiently pure methane. In a recent contribution Romegialli et al. [21]  
103 performed a simulation study with Aspen Plus to estimate the feasibility of ISRU propellant  
104 mass production. The authors included the carbon capture from the Martian atmosphere, the

105 water extraction from martian soil, the methanation and subsequent product purification and  
106 propellant storage in their Aspen model [21]. They state that the total mass required for the  
107 resulting plant design is less than 23% of the 100 metric tons transport capacity of the starship  
108 [21]. Thus, ISRU propellant production should be theoretically possible with the suggested  
109 plant design. While the authors used a Ni/Al<sub>2</sub>O<sub>3</sub> catalyst with LHHW-rate expression for  
110 methanation over Ni-catalysts to model the Sabatier reactor. The effect of the H<sub>2</sub> recycle and  
111 the overstoichiometric H<sub>2</sub>/CO<sub>2</sub> ratio are not evaluated in further detail. Furthermore, Nasa's  
112 research for ISRU propellant production focuses on Ru-based catalysts [3,5,14–16], due to the  
113 higher activity and stability compared to Ni-catalysts [5,22].  
114 Consequently, the focus of the present work is to explore the potential of recycle operation and  
115 non-stoichiometric feed ratios for efficient propellant production on Mars. Therefore, the overall  
116 process is modelled with the major equipment needed. This includes the chemical reactor, the  
117 subsequent separation equipment and the equipment needed for realizing the mass streams.  
118 Emphasis is on exploiting the impact of the H<sub>2</sub>/CO<sub>2</sub> feed ratio and the recycle ratio on the  
119 methane formation rate and the separation effort to achieve a certain product purity.  
120 Thermodynamic modelling is chosen to set the scene as well as to identify the major design  
121 criteria and limitations of the overall process.

## 122 2 Process Concept

123 The considered sub-process of this study is embedded in an overall process scheme, which is  
124 depicted in Figure 1. The energy supply for heating, cooling and work intensive unit operations  
125 is assumed to be secured via solar modules and not further elaborated. The considered  
126 process consists of a methanation reactor, a water separation unit and a gas purification unit  
127 for the product stream and is indicated by a grey box. For providing the complete picture,  
128 storage units, the origin of the raw materials and the energy supply unit for heating, cooling  
129 and providing electrical power for e.g. compressors and the electrolysis are also shown. These  
130 unit operations are not considered in the study (outside grey box). The component streams

131 are colour-coded and connect the individual unit operations. The H<sub>2</sub> and CO<sub>2</sub> recycle streams  
 132 are indicated by dashed lines.



133  
 134 Figure 1: Basic flowsheet of the overall process concept based on [20], the grey box indicates the sub-process  
 135 considered in the present work.

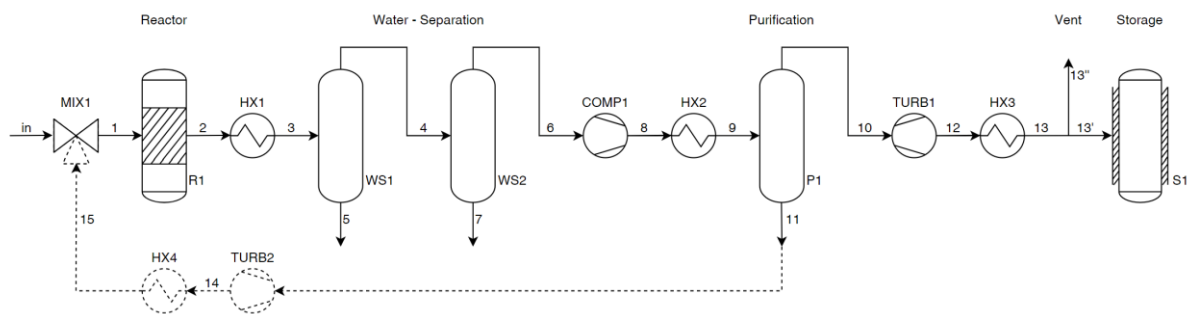
136 In Figure 2 the process flow diagram of the sub-process is depicted in more detail. Two process  
 137 concepts are distinguished: the linear process variant without gas recycle (single pass  
 138 operation, SPO, solid lines) and the variant with gas recycle (recycle operation, RO, additional  
 139 dashed lines). The process consists of a Sabatier reactor (R1), in which the reactions  
 140 according to eqs. (RE1) – (RE3) take place. The conversion  $X_{\text{CO}_2, \text{in} - 2}$  and selectivity  $S_{\text{CH}_4, 1 - 2}$   
 141 of the reactor are defined as follows:

$$X_{\text{CO}_2, \text{in} - 2} = \frac{\dot{n}_{\text{CO}_2, 1} - \dot{n}_{\text{CO}_2, 2}}{\dot{n}_{\text{CO}_2, \text{in}}}, \quad (1)$$

$$S_{\text{CH}_4, 1 - 2} = \frac{\dot{n}_{\text{CH}_4, 2}}{\dot{n}_{\text{CO}_2, 1} - \dot{n}_{\text{CO}_2, 2}}. \quad (2)$$

142 Note that the indices used for the molar flow rates in Eqs. (1) and (2) refer to the stream  
 143 numbers in Figure 2. CO<sub>2</sub> is exclusively transformed into CH<sub>4</sub> and CO through the given  
 144 reaction network (RE1) – (RE3), while the methane selectivity is close to 1. For instance,  
 145 methane selectivities of 99.5% are experimentally observed for supported Ru-catalysts [23–  
 146 25].

147  
 148



149

150 Figure 2: Process flowsheet for the single pass operation (SPO, solid lines) and the recycle operation (RO, solid  
 151 and dashed lines) including key and auxiliary unit operations.

152 Following the chemical conversion water needs to be separated from the product gas stream.

153 This is realized by a two-step setup consisting of a thermodynamic and a mechanical

154 separation unit. Thermodynamic separation is realized by an heat exchanger HX1 to condense

155 water out of the product stream and further reduce its vapor pressure without solidification

156 [26,27]. The subsequent mechanical separation of liquid and gas streams takes place in the

157 water separators WS1 and WS2. Unreacted educts, CO<sub>2</sub> and H<sub>2</sub>, are separated in the

158 purification step P1 via pressure-swing adsorption. In SPO the separated reactants are not

159 utilized and emitted to the Martian atmosphere. In RO the recycled gas stream (11) is

160 combined with the inlet stream (in) in the mixer MIX1 prior to entering the reactor. The

161 produced methane is liquified (stream 13') and stored in a thermally isolated tank S1 including

162 liquid traces of CO<sub>2</sub>, CO and H<sub>2</sub>. The gaseous part of the stream into the storage after HX3 is

163 vented prior entering the tank (stream 13'').

164 Auxiliary unit operations, such as pressure and temperature changers, are modelled using

165 isentropic compressions or expansions, as well as isobaric heating or cooling. They provide

166 the inlet conditions for the adjoining key unit operations.

### 167 3 Simulation

168 For simulation, the process simulator Aspen HYSYS V12.1 is used. The software features a

169 dedicated recycling tool required for the RO setup. Table A1 (in the SI) displays the software's

170 block types used for each unit operation with according pressures and temperatures for the

171 later discussed RO base case scenario (compare section 4.2.). Further HYSYS-flowsheets for  
172 the SPO and RO setup are provided in Figure A1 and A2 (in the SI).

173 Based on the chemical equilibrium of the exothermal gas phase reaction network depicted in  
174 (RE1) – (RE3), the equilibrium reactor R1 is operated isobaric and isothermal at temperatures  
175 and pressures taken from experiments for Ru/Al<sub>2</sub>O<sub>3</sub> catalysed CO<sub>2</sub> methanation [24], as Alam  
176 et al. [5] have done for their reaction conditions. Additionally, the chemical equilibrium  
177 calculation in Aspen HYSYS requires the choice of key reactions which are chosen to be (RE1)  
178 and (RE2).

179 WS1 is modelled as decanter for the mechanical separation of the liquid water rich and  
180 gaseous stream. Subsequently, the remaining water in the gaseous stream, stream 4, is  
181 separated in WS2, which is modelled as an ideal separator set to fully remove the remaining  
182 water. Those water traces can be nearly fully separated by e.g. molecular sieves with  
183 neglectable methane losses of 0.78% and an H<sub>2</sub>O/CH<sub>4</sub> selectivity of 500 [28].

184 The pressure-swing adsorption in P1 is simulated by an ideal separator based on experimental  
185 data: The separation efficiency of CO<sub>2</sub> is set to an efficiency of 94%, while the separation  
186 efficiency for H<sub>2</sub> is set to 87% [5,29,30].

187 According to Aspen HYSYS' user manual, which is accessible via the software itself, the  
188 recycle tool is a theoretical block that iterates until a certain threshold is fulfilled. A sufficiently  
189 high precision has been achieved by setting the number of maximal allowed iterations to 5000,  
190 changing the composition sensitivity from 10 to  $1 \times 10^{-5}$  and all component sensitivities to  
191  $1 \times 10^{-8}$ . The error of the smallest molar flow rate before and after the recycle tool is less than  
192  $1 \times 10^{-6}$  kmol d<sup>-1</sup> (compare  $\dot{n}_{\text{CO}_2}$  in streams 11 and 14 in Table A2 in the SI).

193 The Peng-Robinson equation of state is used as property package in HYSYS for  
194 thermodynamic equilibrium calculations, as it is recommended for systems with high H<sub>2</sub>  
195 fractions [31]. Regarding the model's applicability, the emerging operating conditions are within  
196 the valid ranges of the used thermodynamic model.

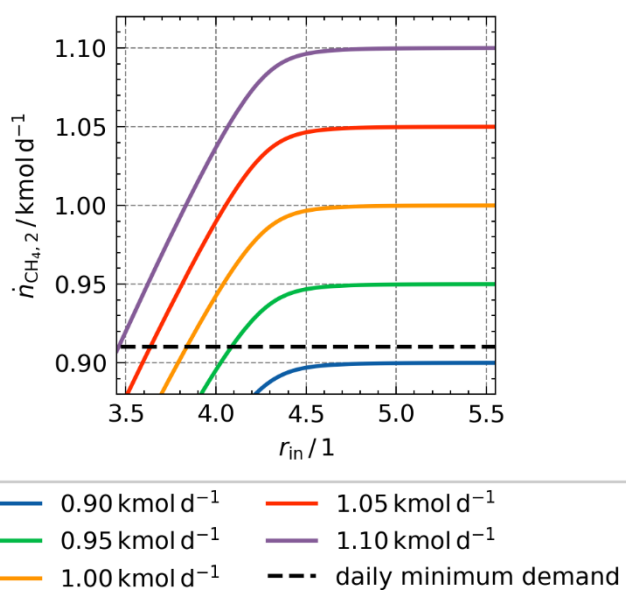
197 To investigate the properties of the process and identify an operation window, parameter  
198 variations are carried out. In case of SPO a variation of the H<sub>2</sub>/CO<sub>2</sub> ratio,  $3.5 \leq r_{\text{in}} \leq 5.5$ , at the

199 reactor inlet (stream (in)) is conducted as well as a variation of the molar flowrate of CO<sub>2</sub>,  
200  $0.9 \text{ kmol d}^{-1} \leq \dot{n}_{\text{CO}_2, \text{in}} \leq 1.1 \text{ kmol d}^{-1}$ , at the reactor inlet. The latter ranges from slightly below  
201 the methane production target of  $0.91 \text{ kmol d}^{-1}$  up to potentially exceeding the production target  
202 by 20%. Note that for SPO the overall inlet stream is identical to the reactor inlet stream.  
203 For RO, the focus is on examining the impact of recycling. Here a variation of the feed stream  
204 composition regarding the H<sub>2</sub>/CO<sub>2</sub> ratio is performed at constant CO<sub>2</sub> inlet molar flow rate.  
205 Hence, the H<sub>2</sub>/CO<sub>2</sub> ratio ranges  $3.5 \leq r_{\text{in}} \leq 5.5$ .

## 206 4 Results

### 207 4.1 Impact of H<sub>2</sub>/CO<sub>2</sub> Feed Ratio in Single Pass Operation

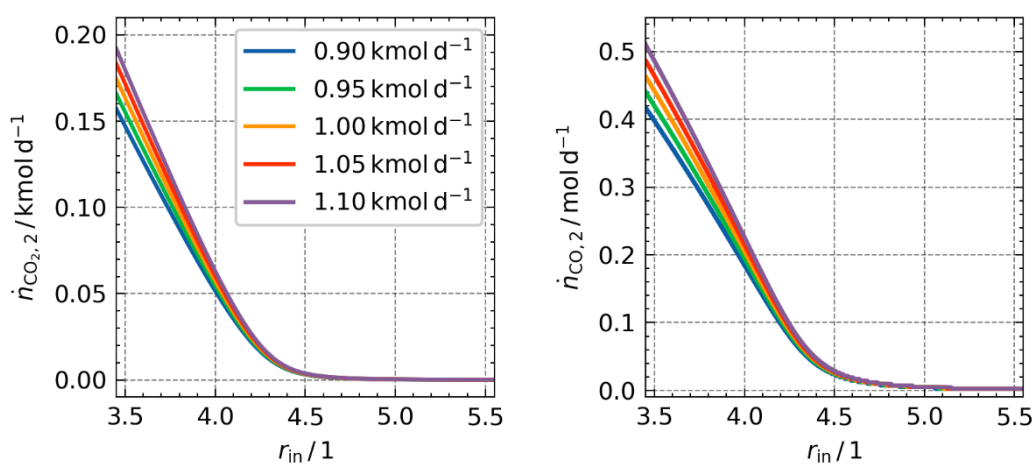
208 The molar flow rate of methane,  $\dot{n}_{\text{CH}_4}$ , at the outlet of the Sabatier reactor (stream 2, see Figure  
209 2) for SPO as function of the inlet H<sub>2</sub>/CO<sub>2</sub> ratio,  $r_{\text{in}}$ , is shown in Figure 3 for various CO<sub>2</sub> inlet  
210 molar flow rates,  $\dot{n}_{\text{CO}_2, \text{in}}$ .



211  
212 Figure 3: CH<sub>4</sub> molar flow rate in stream 2,  $\dot{n}_{\text{CH}_4, 2}$ , as function of H<sub>2</sub>/CO<sub>2</sub> inlet ratio,  $r_{\text{in}}$ , for different CO<sub>2</sub> inlet molar  
213 flow rates,  $\dot{n}_{\text{CO}_2, \text{in}}$ , for SPO.

214 An increase in  $r_{\text{in}}$  results in an increase in the methane molar flow rate until it reaches a  
215 constant value. This general trend is observed for all CO<sub>2</sub> inlet molar flow rates studied, while  
216 the achieved maximum CH<sub>4</sub> flow rate scales with the inlet flow rate of CO<sub>2</sub>. The target CH<sub>4</sub>

217 production rate of  $0.91 \text{ kmol d}^{-1}$ , represented by a dashed horizontal line, requires a sufficient  
 218  $\text{CO}_2$  feed rate depending on conversion and selectivity. Our results show that achieving the  
 219 target requires a minimum inlet flow rate of  $\text{CO}_2$ , which corresponds to the case of full  
 220 conversion and selectivity ( $\dot{n}_{\text{CO}_2,\text{in}} > 0.91 \text{ kmol d}^{-1}$ ). Furthermore, Figure 3 shows that high  
 221  $\text{H}_2/\text{CO}_2$  ratios allow to achieve the target at lower  $\text{CO}_2$  feed rates, while higher  $\text{CO}_2$  feed rates  
 222 are beneficial in cases of small  $\text{H}_2/\text{CO}_2$  ratios. This is expected, since both parameters allow  
 223 to compensate for conversion and selectivity below 100%.  
 224 Regarding the by-products and unreacted reactants at the reactor outlet Figure 4 illustrates  
 225 the molar flow rate of CO and  $\text{CO}_2$  plotted against the  $\text{H}_2/\text{CO}_2$  inlet ratio.



226  
 227 Figure 4: Molar flow rate of  $\text{CO}_2$ ,  $\dot{n}_{\text{CO}_2,2}$ , (a) and CO,  $\dot{n}_{\text{CO},2}$ , (b) as function of the  $\text{H}_2/\text{CO}_2$  inlet ratio,  $r_{\text{in}}$ , for different  
 228  $\text{CO}_2$  inlet flow rates,  $\dot{n}_{\text{CO}_2,\text{in}}$ , for SPO.

229 Both, the  $\text{CO}_2$  and the CO outlet molar flow rates decrease with increasing  $r_{\text{in}}$  and reach zero  
 230 asymptotically. The decrease in  $\text{CO}_2$  flow rate is associated with an increasing conversion,  
 231 while the decrease in CO flow rate indicates a rising  $\text{CH}_4$  selectivity. Both values, conversion  
 232 and selectivity, approach 100% for high values of  $r_{\text{in}}$  (compare Figure 5 and A3 in the SI for  
 233 methane selectivity), which can be attributed to the fact that  $\text{CH}_4$  formation is favoured  
 234 thermodynamically as the  $\text{H}_2/\text{CO}_2$  ratio increases [32]. Consequently, higher  $\text{H}_2/\text{CO}_2$  ratios are  
 235 beneficial for the subsequent  $\text{CH}_4$  purification steps, due to smaller impurity amounts. This  
 236 leads to a decreased equipment size and/or energy demand for methane purification.  
 237 Furthermore, a mass reduction of the unit can be expected, which lowers mission costs,  
 238 especially when considering the high mass-bound transportation costs in space travel [33].

239 These results indicate that operating the SPO process at  $r_{\text{in}} \geq 4.7$  and  $\dot{n}_{\text{CO}_2,\text{in}} \geq 0.91 \text{ kmol d}^{-1}$   
 240 provides nearly full conversion and a selectivity near 1 as well as sufficient production rate  
 241 from thermodynamic perspective. Note that the stoichiometric  $\text{H}_2/\text{CO}_2$  ratio is 4, which means  
 242 that the  $\text{H}_2$  conversion is smaller than the  $\text{CO}_2$  conversion for all cases for which  $\text{H}_2/\text{CO}_2 > 4$ .  
 243 Hence, not only unreacted  $\text{CO}_2$  but also unreacted  $\text{H}_2$  remains in the product stream in those  
 244 cases.

245 For further analysis, we selected  $r_{\text{in}} = 4.7$  and  $\dot{n}_{\text{CO}_2,\text{in}} = 0.91 \text{ kmol d}^{-1}$  as a base case for SPO.  
 246 At the chosen base case, a  $\text{CO}_2$  conversion (Eq. (1)) of 99.89% and a selectivity (Eq. (2)) of  
 247 99.999% is achieved. The impurities entering the storage unit for the SPO base case (see  
 248 Table 1 together with RO results) are sufficiently low to fulfil the fuel Grade A of the US  
 249 department of defence for the performance specification of  $\text{LCH}_4$  (liquified methane) as  
 250 propellant [34]. Thus, our results show, that the required goal in methane productivity of  
 251  $0.91 \text{ kmol d}^{-1}$  can be achieved by employing sufficiently high  $\text{H}_2/\text{CO}_2$  feed ratios in the SPO  
 252 concept without compromising the required fuel purity for applications as propellant with fewer  
 253 unit operations compared to the setup proposed by Alam et al. [20].

254 Table 1: Impurities in liquid stream to storage facility (stream 13') for  $\dot{n}_{\text{CO}_2,\text{in}} = 0.91 \text{ kmol d}^{-1}$ .

$x_{\text{H}_2} / \text{ppm}$	$x_{\text{CO}_2} / \text{ppm}$	$x_{\text{H}_2\text{O}} / \text{ppm}$	$x_{\text{CO}} / \text{ppm}$
SPO, $r_{\text{in}} = 4.7$			
439.48	68.24	0	5.46
RO, $r_{\text{in}} = 4.09$			
439.07	65.55	0	5.45
specification fuel Grade A [34]			
- <sup>1</sup>	125	1	- <sup>1</sup>

255 However, for the SPO unreacted  $\text{H}_2$  with an amount of  $0.641 \text{ kmol d}^{-1}$  is vented with streams  
 256 11 and 13'' (see Table 2 together with RO results).  
 257

<sup>1</sup>other gases (e.g.  $\text{H}_2$ ) must be in total less than 5000 ppm.

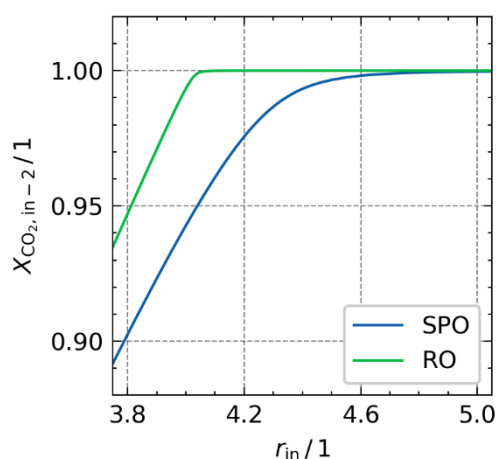
258 Table 2: Vented H<sub>2</sub> in SPO and RO setup with the required  $r_{in,req}$  to meet the set production and purity target @  
 259  $\dot{n}_{CO_2,in} = 0.91 \text{ kmol d}^{-1}$ .

Setup	$r_{in,req}$	H <sub>2</sub> loss in kmol d <sup>-1</sup>	
		stream 11	stream 13''
SPO	4.7	0.558	0.083
RO	4.09	0	0.083

260 Further details about the stream compositions of the remaining streams are provided for the  
 261 RO base case in Table A2 (in the SI).

## 262 4.2 Comparison of Single Pass and Recycle Operation

263 To avoid H<sub>2</sub> venting, the RO scenario is investigated. In Figure 5 the CO<sub>2</sub> conversion (Eq. (1))  
 264 is displayed for the SPO and the RO setup over the respective inlet ratios  $r_{in}$ . In the RO setup  
 265 the trend in CO<sub>2</sub> conversion is similar to that of the SPO. For  $r_{in} < 4$ , H<sub>2</sub> is the stoichiometrically  
 266 limiting component. Hence, even at full H<sub>2</sub> conversion the available CO<sub>2</sub> is only consumed  
 267 stoichiometrically, leading to an increased fraction of CO<sub>2</sub> at the reactor outlet and to the  
 268 recycling of CO<sub>2</sub>. At the same time, CO<sub>2</sub> conversion (Eq. (1)) increases with H<sub>2</sub> availability and  
 269 thereby with  $r_{in}$ . For  $r_{in} > 4$  (stream (in), Figure 2), H<sub>2</sub> is fed in stoichiometric excess, which  
 270 leads to the recycling of unreacted H<sub>2</sub> and an increased CO<sub>2</sub> conversion. Additionally, the  
 271 methane selectivities (Eq. (2)) for both setups are provided in Figure A3 (in the SI).



272  
 273 Figure 5: CO<sub>2</sub> conversion between stream (in) and 2,  $X_{CO_2,in-2}$ , as function of the H<sub>2</sub>/CO<sub>2</sub> inlet ratio  $r_{in}$  @  $\dot{n}_{CO_2,in} =$   
 274  $0.91 \text{ kmol d}^{-1}$  for SPO and RO.

275 As we have shown earlier (see SPO base case), a CO<sub>2</sub> conversion of 99.9% is sufficient to  
 276 fulfil the methane production target and the required purity of fuel grade A. In the SPO setup,

277 this conversion is achieved with setting the ratio  $r_{in}$  to 4.7. In the RO setup, the reactor inlet  
278 ratio  $r_1$  depends on the ratio in the recycle streams,  $r_{15}$ , and the inlet ratio,  $r_{in}$ . Thus, the H<sub>2</sub>/CO<sub>2</sub>  
279 ratio at the reactor inlet (stream 1 in Figure 2) exceeds that at the overall inlet when feeding  
280 H<sub>2</sub> in stoichiometric excess. A ratio  $r_1 = 4.7$  for the RO setup is achieved by setting  $r_{in}$  to 4.09.  
281 By H<sub>2</sub> recycling venting during the purification is avoided, which leads to a significantly reduced  
282 overall H<sub>2</sub> loss (see Table 2), without compromising neither the required conversion for the set  
283 methane production rate nor the fuel purity (see Table 1). From the standpoint of resource  
284 efficiency, it is advantageous to achieve the set production and purity target with smaller  $r_{in}$   
285 values while maintaining the same CO<sub>2</sub> inlet molar flow rate. Therefore, using a recycle stream  
286 renders the RO beneficial in terms of resource consumption, while additional equipment is  
287 needed.

288 It has to be mentioned that we consider the thermodynamic feasible conversion, which  
289 represents the upper bound. For instance, Alam et al. [20] assumed a conversion of 60% (the  
290 authors called it efficiency) at a stoichiometric H<sub>2</sub>/CO<sub>2</sub> ratio of 4 based on kinetic experiments  
291 conducted by Falbo et al. [23]. In equilibrium, we obtain a significantly higher conversion of  
292 approx. 94% at the stoichiometric feed ratio. However, achieving conversions close to  
293 chemical equilibrium is generally viable and a matter of appropriate reactor design as illustrated  
294 by Bremer et al. for adiabatic and polytropic operation strategies [35].

295 Downstream the Sabatier reactor, step-wise product purification is considered. Since water is  
296 formed stoichiometrically with methane, it needs to be separated from the raw product stream,  
297 preferably in the first purification step (WS1 and WS2 in Figure 2). For the SPO base case  
298 ( $r_{in} = 4.7$ ,  $\dot{n}_{CO_2,in} = 0.91 \text{ kmol d}^{-1}$ ), the thermodynamic separation unit achieves a removal  
299 efficiency of 99.62% due to the vapor pressure of water. An additional separation step, e.g. by  
300 adsorption on a molecular sieve [28], would be required to lower the residual water content  
301 further.

### 302 4.3 Potential for Energy Integration

303 In Table 3 the in- and outgoing (negative sign) heat flow rates of all unit operations with the  
304 according temperature levels are given for the SPO and the RO setup. The operating  
305 conditions are chosen according to the previous section:  $\dot{n}_{\text{CO}_2,\text{in}} = 0.91 \text{ kmol d}^{-1}$ ,  $r_{\text{in,SPO}} = 4.7$ ,  
306  $r_{\text{in,RO}} = 4.09$ . There are no noteworthy differences in the heat flow rates and temperature  
307 levels between the both setups. However, due to the recycle in the RO setup, there are some  
308 additional unit operations, namely TURB2 and HX4. Due to the recycling stream preheating in  
309 HX4 prior to the reactor, the overall energy demand is higher for the RO setup. The excess  
310 heat of the unit operations could be used either to provide heat in process steps with heat  
311 demand, like the preheating in HX4, or to heat other systems possibly like the electrolyser or  
312 the human habitat.

313 Table 3: Heat flow rates,  $\dot{Q}$ , for all unit operations (see Figure 2) with temperature levels for the SPO (top line) and  
314 the RO (bottom line) setup @  $\dot{n}_{\text{CO}_2,\text{in}} = 0.91 \text{ kmol d}^{-1}$ ,  $r_{\text{in,SPO}} = 4.7$ ,  $r_{\text{in,RO}} = 4.09$  as well as temperature levels on  
315 Mars.

Unit Operation	$\dot{Q} / \text{W}$	$T_{\text{max}} / \text{K}$	$T_{\text{min}} / \text{K}$
R1	-1868.3	309.9	309.9
	-1870.3	309.9	309.9
HX4	-	-	-
	57.5	309.9	1.9
HX1	-1384.4	309.9	0
	-1386.1	309.9	0
COMP1	17.5	29.9	0
	17.5	29.9	0
HX2	-5.3	29.9	21.0
	-5.3	29.9	21.0
P1	-0.1	21.0	21.0
	-0.1	21.0	21.0
TURB1	-6.5	21.0	4.5
	-6.5	21.0	4.5

	-	-	-
TURB2	-3.5	21.0	1.9
WS1	0	0	0
WS2	-3.6	0	0
HX3	-154.3	4.5	-173.2
Mars	20	-90	

#### 316 4.4 Considerations on site selection

317 The preceding section illustrates that downstream processing can be minimized by employing  
318 excess hydrogen at the reactor feed for both the SPO and RO configurations. In the SPO  
319 configuration, an inlet ratio of  $r_{in,SPO} = 4.7$  is to achieve the set objectives for purity as well as  
320 production rate, while  $r_{in,RO} = 4.09$  is sufficient for the RO. Due to the different H<sub>2</sub> demand of  
321 the two suggested setups, the availability of hydrogen at a given landing site may determine  
322 whether a recycle is necessary or not.

323 Sites with abundantly available water (and H<sub>2</sub>) resources probably profit from using the simpler  
324 SPO concept, which comes along with higher hydrogen consumption. Main advantage is that  
325 the required number of unit operations and equipment is low, while excess hydrogen is purged  
326 into the atmosphere or used for energy generation. However, sites with scarce availability of  
327 H<sub>2</sub>, may profit from its efficient usage, for which the RO concept with lower hydrogen  
328 consumption is beneficial. However, this process variant entails additional equipment, which  
329 increases weight, transport costs, process complexity, and the risk of failure.

330 Considering the mission scenarios outlined in the introduction, the decision for single or  
331 multiple landing sites affects the process configuration choice. For a single landing site, where  
332 multiple crews will subsequently be present, it is likely that water and thus hydrogen are  
333 abundant. Therefore, the SPO concept is the preferred choice due to its potential higher  
334 reliability, lower weight, and transportation costs. The RO variant may be preferred for

335 continuous long-term operation at a single landing site, due to its efficient H<sub>2</sub> utilization. The  
336 higher process complexity associated higher weight and transport costs, may be  
337 overcompensated by the process efficiency and flexibility.

338 In the case of multiple landing sites, the sufficient availability of water may not be guaranteed  
339 at each single site. Hence, the RO concept is the preferred process variant as it is more flexible  
340 and requires less water resources. Only the higher complexity may contrast that  
341 recommendation.

## 342 5 Conclusion

343 The present work introduces and compares promising process concepts for *in situ* methanation  
344 on Mars based on an extensive simulation study. Specifically, we propose to optimize the  
345 H<sub>2</sub>/CO<sub>2</sub> ratio and the recycle of unreacted H<sub>2</sub> and CO<sub>2</sub> species, to minimize the process  
346 complexity and product purification efforts. We found that H<sub>2</sub>/CO<sub>2</sub> ratios above the  
347 stoichiometric value of 4 are beneficial, since practically full conversion and selectivity can be  
348 achieved. This minimizes the amount of unconverted reactants and byproducts for  
349 downstream processing and thereby the process complexity. The remaining separation of CH<sub>4</sub>  
350 and H<sub>2</sub> is feasible in principle and modelled by a thermodynamic approach.

351 One degree of freedom in process design is the potential recycle of unconverted reactants.  
352 While it offers an improved utilization of H<sub>2</sub>, which is especially important in cases with scarce  
353 availability of water, it comes along with higher process complexity. Hence, the mass and  
354 associated inter-planetary transportation costs are higher, as well. At the same time, the  
355 recycle concept is more flexible in operations. Consequently, both proposed process variants,  
356 the SPO and the RO, are attractive options for ISRU methanation.

357 The results of our study show that propellant production on Mars is possible via two promising  
358 process concepts depending and the specific site and scenario. Since our results are based  
359 on thermodynamic modelling, only, additional kinetic investigations are needed for sizing and  
360 estimating the mass of the major equipment in upcoming work. Therefore, combination of  
361 simulations with experimental investigations establish the basis for more detailed concepts of

362 the unit operations. One of the major design criterions, beside the mass of the overall unit, are  
363 the robustness of the process and the ability to provide the required propellant purity.  
364 Therefore, the present study provides insights into potential degrees of freedom for process  
365 design, that is the H<sub>2</sub>/CO<sub>2</sub> feed and the recycle ratio.

366

367

368

### 369 **Symbols used**

<b>Symbol</b>	<b>Unit</b>	<b>Description</b>
$\dot{n}_i$	kmol d <sup>-1</sup>	Molar flow rate of component <i>i</i>
$p$	bar	Pressure
$r$	1	H <sub>2</sub> /CO <sub>2</sub> ratio
$S_{\text{CH}_4}$	1	Selectivity
$T$	K	Temperature
$x$	1	Molar fraction
$X_{\text{CO}_2}$	1	CO <sub>2</sub> -Conversion

370

### 371 **Abbreviations**

<b>Abbreviation</b>	<b>Definition</b>
DMR	Design Reference Mission
ERV	Earth return vehicle
ISRU	<i>In Situ</i> Resource Utilization
ISS	International Space Station
LCH <sub>4</sub>	Liquified methane
MARCO	Mars Atmospheric and
POLO	Regolith Collector/Processing for Lander Operations
MAV	Mars ascent vehicle
MOXIE	Mars Oxygen In-Situ Resource Utilization
PR	Peng-Robinson
RO	Recycle operation
SPO	Single pass operation

372

## 373 Supporting Information

374 Supporting Information are provided, which include the model parameters and flow sheets for  
375 simulation as well as detailed results.

## 376 References

- 377 [1] NASA, Human Exploration of Mars Design Reference Architecture 5.0 Addendum, (2009).  
378 [https://www.nasa.gov/pdf/373667main\\_NASA-SP-2009-566-ADD.pdf](https://www.nasa.gov/pdf/373667main_NASA-SP-2009-566-ADD.pdf) (accessed August 20,  
379 2024).
- 380 [2] G.F. Acosta, A. Scott, A. Jason, D. Matt, H. Matt, K. Jared, K. Takahasi, M. Mohrli, M. Karen, M.  
381 Mark, P. Daniel, T. Norihito, T. Igor, W. Chris, Y. Keith, Project Genesis: Mars in Situ Propellant  
382 Technology Demonstrator Mission, (2009).  
383 <https://ntrs.nasa.gov/api/citations/19950006409/downloads/19950006409.pdf> (accessed  
384 February 04, 2025).
- 385 [3] NASA, Human Exploration of Mars Design Reference Architecture 5.0, (2009).  
386 [https://www.nasa.gov/wp-content/uploads/2015/09/373665main\\_nasa-sp-2009-  
387 566.pdf?emrc=6dfe40](https://www.nasa.gov/wp-content/uploads/2015/09/373665main_nasa-sp-2009-566.pdf?emrc=6dfe40) (accessed August 20, 2024).
- 388 [4] NASA, Human Exploration of Mars Design Reference Architecture 5.0 Addendum, (2009).  
389 [https://www.nasa.gov/pdf/373667main\\_NASA-SP-2009-566-ADD.pdf](https://www.nasa.gov/pdf/373667main_NASA-SP-2009-566-ADD.pdf) (accessed August 20,  
390 2024).
- 391 [5] S.S. Alam, C. Depcik, S.P. Burugupally, J. Hobeck, E. McDaniel, Thermodynamic modeling of  
392 in-situ rocket propellant fabrication on Mars, *iScience* 25 (2022) 104323.  
393 <https://doi.org/10.1016/j.isci.2022.104323>.
- 394 [6] S. Rönsch, J. Schneider, S. Matthischke, M. Schlüter, M. Götz, J. Lefebvre, P. Prabhakaran, S.  
395 Bajohr, Review on methanation – From fundamentals to current projects, *Fuel* 166 (2016) 276–  
396 296. <https://doi.org/10.1016/j.fuel.2015.10.111>.
- 397 [7] W.J. Lee, C. Li, H. Prajitno, J. Yoo, J. Patel, Y. Yang, S. Lim, Recent trend in thermal catalytic  
398 low temperature CO<sub>2</sub> methanation: A critical review, *Catal. Today* 368 (2021) 2–19.  
399 <https://doi.org/10.1016/j.cattod.2020.02.017>.
- 400 [8] B. Höhle, H. Niessen, J. Range, H.J.R. Schiebahn, M. Vorwerk, Methane from synthesis gas  
401 and operation of high-temperature methanation, *Nucl. Eng. Des.* 78 (1984) 241–250.  
402 [https://doi.org/10.1016/0029-5493\(84\)90308-X](https://doi.org/10.1016/0029-5493(84)90308-X).
- 403 [9] S. Matthischke, S. Roensch, R. Güttel, Start-up Time and Load Range for the Methanation of  
404 Carbon Dioxide in a Fixed-Bed Recycle Reactor, *Ind. Eng. Chem. Res.* 57 (2018) 6391–6400.  
405 <https://doi.org/10.1021/acs.iecr.8b00755>.
- 406 [10] S. Theurich, S. Rönsch, R. Güttel, Transient Flow Rate Ramps for Methanation of Carbon  
407 Dioxide in an Adiabatic Fixed-Bed Recycle Reactor, *Energy Technol.* 8 (2020) 1901116.  
408 <https://doi.org/10.1002/ente.201901116>.
- 409 [11] C. Junaedi, K. Hawley, D. Walsh, S. Roychoudhury, M. Abney, J. Perry, Compact and  
410 Lightweight Sabatier Reactor for Carbon Dioxide Reduction, in: 41st Int. Conf. Environ. Syst.,  
411 American Institute of Aeronautics and Astronautics, Portland, Oregon, 2011.  
412 <https://doi.org/10.2514/6.2011-5033>.
- 413 [12] L.M. Romeo, M. Cavana, M. Bailera, P. Leone, B. Peña, P. Lisbona, Non-stoichiometric  
414 methanation as strategy to overcome the limitations of green hydrogen injection into the natural  
415 gas grid, *Appl. Energy* 309 (2022) 118462. <https://doi.org/10.1016/j.apenergy.2021.118462>.
- 416 [13] T.T. Chen, Integrated Simulations of the Sabatier and Carbon Vapor Deposition Reactor to  
417 Understand Its Impacts to Operations and Performance, (2024).  
418 <https://ntrs.nasa.gov/api/citations/20240004053/downloads/ICES-2024-156-Final.pdf>.
- 419 [14] S.O. Starr, A.C. Muscatello, Mars in situ resource utilization: a review, *Planet. Space Sci.* 182  
420 (2020) 104824. <https://doi.org/10.1016/j.pss.2019.104824>.
- 421 [15] Anthony C. Muscatello, Paul E. Hintze, Anne J. Meier, Elspeth M. Petersen, Jon A. Bayliss,  
422 Ricardo M. Gomez Cano, Rene Formoso, Malay G. Shah, Jared J. Berg, Bruce T. Vu, Alexander  
423 R. Walts, Rupert U. Lee, Rene Formoso, Malay G. Shah, Jared J. Berg, Bruce T. Vu, Alexander  
424 R. Walts, Rupert U. Lee, James G. Captain, Testing and Modeling of the Mars Atmospheric

- 425 Processing Module, AIAA SPACE Astronaut. Forum Expo. (2017).  
426 <https://doi.org/10.2514/6.2017-5149>.
- 427 [16] A.J. Meier, M.G. Shah, P.E. Hintze, E. Petersen, Mars Atmospheric Conversion to Methane and  
428 Water: An Engineering Model of the Sabatier Reactor with Characterization of Ru/Al<sub>2</sub>O<sub>3</sub> for Long  
429 Duration Use on Mars, 47th Int. Conf. Environmental Syst. (2017).  
430 <https://ntrs.nasa.gov/api/citations/20170007818/downloads/20170007818.pdf>.
- 431 [17] F. Smith, J. Perry, K. Murdoch, L. Goldblatt, Sabatier Carbon Dioxide Reduction Assembly  
432 Development for Closed Loop Water Recovery, (2004).  
433 <https://ntrs.nasa.gov/api/citations/20100033195/downloads/20100033195.pdf>.
- 434 [18] J.A. Hoffman, M.H. Hecht, D. Rapp, J.J. Hartvigsen, J.G. SooHoo, A.M. Aboobaker, J.B.  
435 McClean, A.M. Liu, E.D. Hinterman, M. Nasr, S. Hariharan, K.J. Horn, F.E. Meyen, H. Okkels, P.  
436 Steen, S. Elangovan, C.R. Graves, P. Khopkar, M.B. Madsen, G.E. Voecks, P.H. Smith, T.L.  
437 Skafte, K.R. Araghi, D.J. Eisenman, Mars Oxygen ISRU Experiment (MOXIE)—Preparing for  
438 human Mars exploration, *Sci. Adv.* 8 (2022) eabp8636. <https://doi.org/10.1126/sciadv.abp8636>.
- 439 [19] R. Šeško, K. Lambole, T. Cutard, L. Grill, P. Reiss, A. Cowley, Oxygen production by solar  
440 vapor-phase pyrolysis of lunar regolith simulant, *Acta Astronaut.* 224 (2024) 215–225.  
441 <https://doi.org/10.1016/j.actaastro.2024.08.009>.
- 442 [20] S.S. Alam, C. Depcik, S.P. Burugupally, J. Hobeck, E. McDaniel, Thermodynamic modeling of  
443 in-situ rocket propellant fabrication on Mars, *iScience* 25 (2022) 104323.  
444 <https://doi.org/10.1016/j.isci.2022.104323>.
- 445 [21] S. Romegialli, A. Tripodi, A. Gramegna, M. Tommasi, G. Ramis, I. Rossetti, Production of  
446 Synthetic Methane for Aerospace Applications: A Mars Case, *Ind. Eng. Chem. Res.* 64 (2025)  
447 190–208. <https://doi.org/10.1021/acs.iecr.4c03411>.
- 448 [22] S. Rönsch, J. Schneider, S. Matthischke, M. Schlüter, M. Götz, J. Lefebvre, P. Prabhakaran, S.  
449 Bajohr, Review on methanation – From fundamentals to current projects, *Fuel* 166 (2016) 276–  
450 296. <https://doi.org/10.1016/j.fuel.2015.10.111>.
- 451 [23] L. Falbo, C.G. Visconti, L. Lietti, J. Szanyi, The effect of CO on CO<sub>2</sub> methanation over Ru/Al<sub>2</sub>O<sub>3</sub>  
452 catalysts: a combined steady-state reactivity and transient DRIFT spectroscopy study, *Appl.*  
453 *Catal. B Environ.* 256 (2019) 117791. <https://doi.org/10.1016/j.apcatb.2019.117791>.
- 454 [24] L. Falbo, M. Martinelli, C.G. Visconti, L. Lietti, C. Bassano, P. Deiana, Kinetics of CO<sub>2</sub>  
455 methanation on a Ru-based catalyst at process conditions relevant for Power-to-Gas  
456 applications, *Appl. Catal. B Environ.* 225 (2018) 354–363.  
457 <https://doi.org/10.1016/j.apcatb.2017.11.066>.
- 458 [25] G. Baade, J. Friedland, K. Ray, R. Güttel, CO<sub>2</sub> hydrogenation on ruthenium: comparative study  
459 of catalyst supports, *RSC Sustain.* 2 (2024) 3826–3834. <https://doi.org/10.1039/D4SU00469H>.
- 460 [26] D.R. Douslin, Vapor pressure of water from –2.5 to 20°C, *J. Chem. Thermodyn.* 3 (1971) 187–  
461 193. [https://doi.org/10.1016/S0021-9614\(71\)80101-5](https://doi.org/10.1016/S0021-9614(71)80101-5).
- 462 [27] P. Linstrom, NIST Chemistry WebBook, NIST Standard Reference Database 69, (1997).  
463 <https://doi.org/10.18434/T4D303>.
- 464 [28] H. Lin, S.M. Thompson, A. Serbanescu-Martin, J.G. Wijmans, K.D. Amo, K.A. Lokhandwala, B.T.  
465 Low, T.C. Merkel, Dehydration of natural gas using membranes. Part II: Sweep/countercurrent  
466 design and field test, *J. Membr. Sci.* 432 (2013) 106–114.  
467 <https://doi.org/10.1016/j.memsci.2012.12.049>.
- 468 [29] S. Sircar, T.C. Golden, Purification of Hydrogen by Pressure Swing Adsorption, *Sep. Sci.*  
469 *Technol.* 35 (2000) 667–687. <https://doi.org/10.1081/SS-100100183>.
- 470 [30] S. Sircar, W.C. Kratz, Simultaneous Production of Hydrogen and Carbon Dioxide from Steam  
471 Reformer Off-Gas by Pressure Swing Adsorption, *Sep. Sci. Technol.* 23 (1988) 2397–2415.  
472 <https://doi.org/10.1080/01496398808058461>.
- 473 [31] J. Haydary, *Chemical Process Design and Simulation: Aspen Plus and Aspen Hysys*  
474 *Applications*, 1st ed., Wiley, 2018. <https://doi.org/10.1002/9781119311478>.
- 475 [32] A. Kakoe, A. Ghareghani, Carbon oxides methanation in equilibrium; a thermodynamic  
476 approach, *Int. J. Hydrog. Energy* 45 (2020) 29993–30008.  
477 <https://doi.org/10.1016/j.ijhydene.2020.08.073>.
- 478 [33] D. Rapp, *Use of Extraterrestrial Resources for Human Space Missions to Moon or Mars*,  
479 Springer Berlin Heidelberg, Berlin, Heidelberg, 2013. <https://doi.org/10.1007/978-3-642-32762-9>.
- 480 [34] J. Baker, R. Khaleel Rahman, R. Olivera, S. Vasu, Assessment of impurities effect on  
481 methane/natural gas ignition at high pressure, in: *AIAA SCITECH 2023 Forum*, American  
482 Institute of Aeronautics and Astronautics, National Harbor, MD & Online, 2023.  
483 <https://doi.org/10.2514/6.2023-2378>.
- 484 [35] J. Bremer, K. Sundmacher, Novel Multiplicity and Stability Criteria for Non-Isothermal Fixed-Bed  
485 Reactors, *Front. Energy Res.* 8 (2021) 549298. <https://doi.org/10.3389/fenrg.2020.549298>.

486 **Credit:**  
487 Franz Braun, Samuel Prinz, Thomas-Oliver Nagel: Methodology, Investigation, Data curation,  
488 Writing original draft, Visualization, Writing review & editing  
489 Jens Friedland: Conceptualization, Methodology, Investigation, Supervision, Project  
490 administration, Writing review & editing  
491 Robert Güttel: Resources, Conceptualization, Methodology, Investigation, Supervision, Project  
492 administration, Writing review & editing